Avrupa Bilim ve Teknoloji Dergisi
Özel Sayı, 34, S. 800-804, Mart 2022
© Telif hakkı EJOSAT'a aittir
Araştırma Makalesi

www.ejosat.com ISSN:2148-2683

European Journal of Science and Technology
Special Issue 34, pp. 800-804, March 2022
Copyright © 2022 EJOSAT
Research Article

Evaluation of the Pressure and Wall Shear Stress on the Aneurysm Wall According to the Growth Position of a Femoral Artery Pseudoaneurysm by Numerical Analysis

Gökhan Keskin[1*], Ahmet Turan Kaya[2]

[1*] Amasya University, Faculty of Medicine, Department of Cardiology, Amasya, Turkey, (ORCID: 0000-0002-1695-5624), keskinand@gmail.com
[2] Sabuncuoğlu Şerefeddin Research and Education Hospital, Department of Radiology, Amasya, Turkey, (ORCID: 0000-0001-9803-453x), hmttrnky.62@gmail.com

(First received 19 February 2022 and in final form 16 March 2022)

(**DOI:** 10.31590/ejosat.1076137)

ATIF/REFERENCE: Keskin, G., Kaya, A.T. (2022). Evaluation of the Pressure and Wall Shear Stress on the Aneurysm Wall According to the Growth Position of a Femoral Artery Pseudoaneurysm by Numerical Analysis *European Journal of Science and Technology*, (35), 800-804.

Abstract

In this study, the effect of the angle change between the neck region and the aneurysm region of a femoral artery pseudoaneurysm (β) on the pressure and shear stresses on the aneurysm wall was investigated with the computational fluid dynamics (CFD) method. The CFD method is an important tool in observing the direction and velocity of blood flow. With the numerical analysis results, it was aimed to evaluate the growth rate and rupture risk of the aneurysm. Findings obtained as a result of the change of β angle between 0˚ and 15˚ for a certain value of the angle between the femoral artery and the aneurysm neck region (α=45˚) were presented in graphs containing velocity vectors inside the aneurysm, pressure, and wall shear stresses on the aneurysm wall. When all the analysis results were evaluated, it was understood that for a pseudoaneurysm formed in the femoral artery, the highest growth rate and risk of rupture could occur at the β =0˚ angle. It was predicted that the obtained findings will be beneficial in determining the treatment method and time in the treatment of femoral artery pseudoaneurysm.

Keywords: Pressure, Pseudoaneurysm, Wall shear stress.

Femoral Arter Psödoanevrizma Büyüme Pozisyonuna Göre Anevrizma Duvarındaki Basınç ve Duvar Kayma Gerilmesinin Sayısal Analiz ile Değerlendirilmesi

Öz

Bu çalışmada femoral arter psödoanevrizmasında (β) boyun bölgesi ile anevrizma bölgesi arasındaki açı değişiminin anevrizma duvarındaki basınç ve kayma gerilmelerine etkisi hesaplamalı akışkanlar dinamiği (HAD) yöntemi ile araştırıldı. CFD yöntemi, kan akışının yönünü ve hızını gözlemlemede önemli bir araçtır. Sayısal analiz sonuçları ile anevrizmanın büyüme hızı ve rüptür riskinin değerlendirilmesi amaçlandı. Femoral arter ile anevrizma boyun bölgesi arasındaki açının belirli bir değeri (α=45˚) için β açısının 0˚ ile 15˚ arasında değişmesi sonucu elde edilen bulgular, anevrizma içindeki hız vektörlerini içeren grafiklerde sunuldu, anevrizma duvarındaki basınç ve duvar kayma gerilmeleri. Tüm analiz sonuçları değerlendirildiğinde femoral arterde oluşan psödoanevrizma için en yüksek büyüme hızı ve rüptür riskinin β =0˚ açısında olabileceği anlaşıldı. Elde edilen bulguların femoral arter psödoanevrizma tedavisinde tedavi yöntemi ve süresinin belirlenmesinde faydalı olacağı öngörülmüştür.

Anahtar Kelimeler: Basınç, Psödoanevrizma, Duvar kayma gerilimi.

* Corresponding Author: keskinand@gmail.com

1. Introduction

Arterial complications possess a known risk area for diagnosis and therapy during the cardiological and radiological procedures. The complications consist of bleeding, dissection, infection, thromboembolism, arteriovenous fistula, and arterial pseudoaneurysm (McCann et all., 1991, Kronzon 1997). The most common site of access to the arterial system and the left side of the heart is the femoral artery. The general technique is percutaneous artery cannulation or a modification thereof, relative to the Seldinger technique. Arterial bleeding is controlled by direct pressure at the end of the intervention after the removal of catheters. Pseudoaneurysms are localized pulsatile mass structures that are formed by the blood coming out of the arterial lumen because of the deterioration of the arterial wall and at the same time communicating with the lumen. Moreover, pseudoaneurysm is the most encountered complication of femoral artery catheterization procedure (Kronzon 1997).

With a high incidence of 2.9%, femoral artery pseudoaneurysm (FAP) is a commonly experienced complication after endovascular intervention (Hirano et all., 2004). Currently, the standard treatment for FAP includes inserting a needle with the aid of an ultrasound probe into the sac where the thrombin is injected, and ultrasound-guided injection of thrombin (UGTI) to induce thrombosis and close the defect in the lumen (Cope et all., 1986). Even though this intervention saves the patient from the morbidity related with open surgical repair, it does not eliminate all complications that can arise after UGTI (Franco et all., 1993, Lumsden et all., 1994). The complications of UGTI may include acute limb ischemia due to distal embolization. Moreover, as UGTI does not always finalize successfully at the first attempt and may require re-injection or surgical repair (Yoo et all., 2017, Stone et all., 2014).

Analyzing blood flow with the computational fluid dynamics method is an essential tool to observe the direction and velocity of blood flow in an aneurysm. On the other hand, with this method, the pressure and the blood flow-originated wall shear stress on the aneurysm wall can be determined. There are only two numerical studies present in the literature for the femoral pseudoaneurysm. Suh et al. investigated the effect of the angle between the aneurysm neck and the femoral artery on the pressure created by the blood flow on the aneurysm wall (Suh S et all., 2012). Kim et al. performed a numerical study to identify the location and time of percutaneous thrombin injection for different pseudoaneurysm sizes with a right-angled neck (Kim H et all., 2021). Unlike studies in the literature, in this study, the effect of the angle between the neck region of the pseudoaneurysm and the aneurysm on the pressure and wall shear stresses inside the aneurysm was examined. The blood flow was modeled numerically, and the conservation equations were solved in three dimensions and time dependent. With the numerical analyzes performed, the growth rate and rupture risk were tried to be evaluated according to the stance position of the pseudoaneurysm.

2. Physical problem and Mathematical model

Patient-specific clinical data in Ref. 9 (Suh S et all., 2012) were used for the pseudoaneurysm considered in this study. The CT angiography image of the pseudoaneurysm is given in Fig. 1. Fig. 2, on the other hand, shows the ideal model of the pseudoaneurysm created for the numerical analysis in this study. Numerical analyzes were performed for different values of the angles of the pseudoaneurysm neck with the femoral artery (α) and the angles of the pseudoaneurysm with the neck region (β). The values of α and β angles used for numerical analysis are given in Table 1.

Eq. (1) and (2) implicate the mass and momentum conservation equations for the blood under laminar conditions, respectively,

$$\nabla . v = 0 \tag{1}$$

$$\rho(\frac{dv}{dt} + v.\nabla v) = -\nabla P + \mu \nabla^2 v \tag{2}$$

Table 1. Parameter values

Angles	α=45°
β	0°
	10°
	15°

In these equations, indicates the velocity vector, (1060 kg/m^3) denotes the density of blood, while and P indicate the dynamic viscosity of blood and pressure, respectively. Viscosity is a function of shear rate (γ) in the function and is not a constant. Eq. (3) defines the dynamic viscosity (Carreu model),

$$\mu(\dot{\gamma}) = \mu_\infty + (\mu_0 - \mu_\infty)[1 + (\lambda \dot{\gamma})^2]^{\frac{n-1}{2}} \tag{3}$$

The Blood flow coefficients shown in Eq. 3 are as follows (Shojima M et all. 2004),

$$\mu_0 = 0,056 (kg / m.s)$$
$$\mu_\infty = 0.0035 (kg / m.s)$$
$$\lambda = 3.313 (s)$$
$$n = 0.3568$$

In this equation, μ_0 and μ_∞ denote the dynamic viscosity at zero and high shear rates, respectively, while λ and n are the coefficients.

In order to simplify the study, the assumption of non-slip condition on blood vessel walls was made and the blood vessels were considered rigid (Siebert et all., 2009, Qiu et all., 2013) For the numerical analysis, velocity values measured by a patient was used for the time-dependent inlet and outlet velocity profiles of the blood flow. These velocity profiles are used as inlet and outlet boundary conditions for numerical analysis. Time-dependent velocity profiles used in this numerical study are indicated in Fig. 3.

Figure 1. The CT angiography image of the pseudoaneurysm [9]

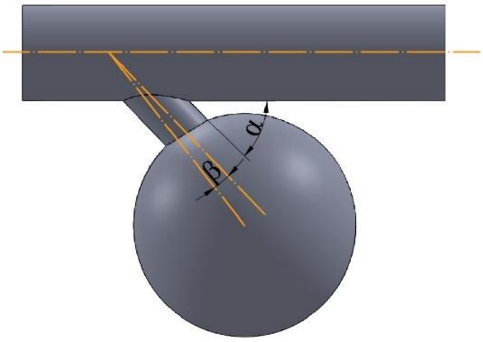

Figure 2. The ideal model of the pseudoaneurysm

a)

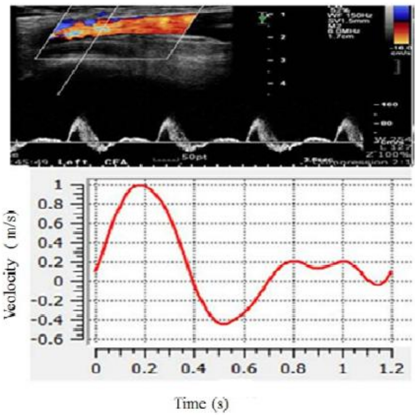

b)

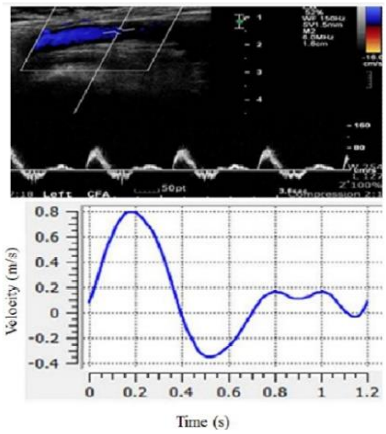

Figure 3. A patient′s velocity profile during a cardiac cycle (Suh H et all., 2012) a) Velocity curve at the inlet b) Velocity curve at the outlet

2.1. Numerical methods

The finite volume method was employed for numerical solutions and calculations were carried out by using ANSYS-Fluent software (Kurşun et all., 2018). SIMPLE algorithm was employed to solve the pressure-velocity coupling. The second order UPWIND scheme was used to discretize and solve the continuity, momentum, and energy equations. Also, the Carreu model indicated in Eq. (3) was employed to determine the velocity-dependent viscosity. The convergence criterion for the mass and momentum conservation equations is expressed by Eq. (5).

$$\left| \frac{\delta^{n+1}(i,j,k) - \delta^{n}(i,j,k)}{\delta^{n+1}(i,j,k)} \right| < 10^{-5} \tag{5}$$

In Eq. (5), and   denote the two consecutive iterations, while δ is any variable, and i, j and k are the grid locations at the direction of x, y, and z axes, respectively.

2.2. Numerical result validation

To validate the numerical results, a comparison was made with Doppler velocity images of a patient in Suh H et all., 2012. Validation was done for the blood velocity values in the pseudoaneurysm. Unstructured grid structure was used in the computational domain (Fig. 4). In computational region, the grid structure was tightened so that the velocity boundary layer formation can be accurately detected in regions close to vessel and aneurysm walls. The velocity values in the pseudoaneurysm obtained as a result of the numerical analysis in Suh H et all., 2012 were compared with the velocity values in the Doppler ultrasound image of a patient and the accuracy of the numerical model was demonstrated. Therefore, the numerical results in this study were compared with the numerical results in Suh H et all., 2012. In Fig. 5 shows the comparison of velocity vectors in the femoral artery and inside the pseudoaneurysm. As seen in Fig. 5, the velocity profile and velocity values within the aneurysm are quite similar. In both studies, the highest flow velocity occurred in the neck region of the aneurysm and reached 1.46 m/s. These results revealed that the numerical model used in this study can be used for the hemodynamic analysis of blood flow within the pseudoaneurysm.

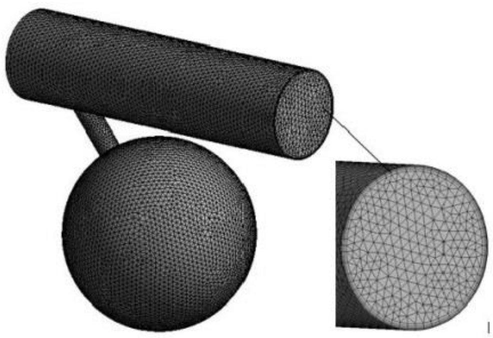

Figure 4. Mesh structure for pseudoaneurysm mode

a)

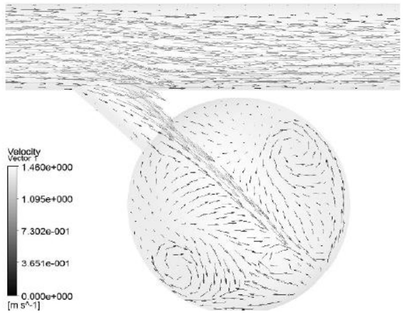

b)

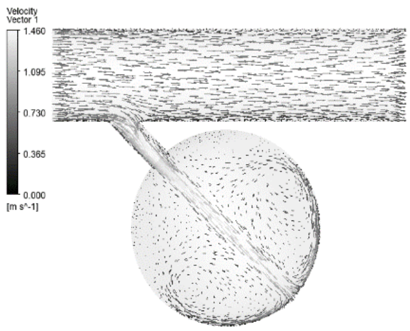

Figure 5. Velocity vectors in the midplane (0.31 s) a) the study by Suh et al. [9] b) the present study

3. Results and Discussions

Although surgery gives the most definitive results in the treatment of femoral pseudoaneurysm, its most important disadvantage is that it is invasive. Thrombin injection method can also be widely preferred among the treatment options because it is less invasive than surgery and has a high success rate in the treatment (Launder et all., 2013). Although it is very easy to apply, the thrombin injection method always carries a risk of thromboembolism. Also, the shear stress and pressure occur on the aneurysm walls have a great effect on the growth rate of the pseudoaneurysm and the increase in the risk of rupture (Krueger et all., 2005). In current study, we investigated the blood flow in the aneurysm and pressure and shear stresses on the aneurysm wall depending on the position of the pseudoaneurysm. The analyzes made it possible to interpret the growth rate and rupture risk of the pseudoaneurysm and to identify the conditions with a high risk of thromboembolism. Numerical analyses were performed for different values of the angles of the pseudoaneurysm neck with the femoral artery (α) and the angles of the pseudoaneurysm with the neck region (β).

In Fig. 6, 7, and 8, velocity vectors, pressure, and shear stress contours at different angles between the aneurysm and neck (β=0˚, 10˚, and 15˚) were given for the case where the angle between the aneurysm neck and the femoral artery was α=45˚. Pressure and shear stresses on the surface of the aneurysm were examined for the peak point of the cardiac cycle (0.2 s). The highest velocity in the neck region of the pseudoaneurysm occurred for the β=0˚ angle (2.328 m/s). The increase in the velocity in the neck region caused an increase in the pressure on the aneurysm surface. Therefore, the highest-pressure value (15116.6 Pa) in the aneurysm dome was obtained for the β=0˚ angle (Fig. 6). At other β angle values (10˚and 15˚), the fluid entering the aneurysm followed the surface of the aneurysm and created a vortex, thus reducing the velocity of blood flow from the neck region. Thus, lower pressure values occurred in the aneurysm dome for β=10˚ and β=15˚ values. When Figs. 6, 7 and 8 are examined, it was observed that the wall shear stress values decrease the increased values of β angle. While increasing from β=0˚ to β=15˚, the maximum wall shear stress value decreased from 87.7 Pa to 48.2 Pa. The reason for the decrease in the wall shear stresses was the decrease in the velocity and pressure of the fluid hitting the aneurysm surface as mentioned above.

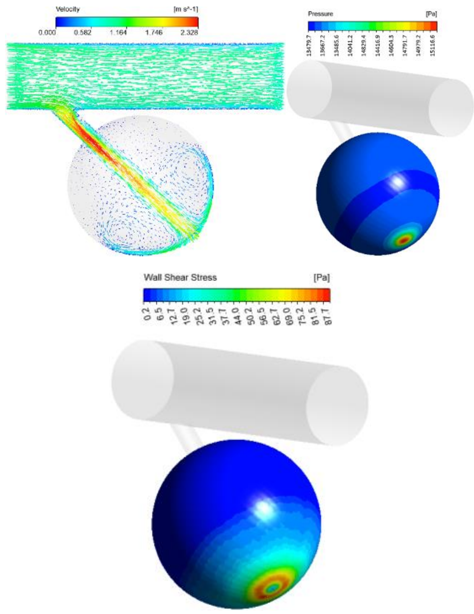

Figure 6. Velocity vectors in the midplane, pressure and wall shear stress on the aneursym surface (α=45˚, β=0˚, t=0.2 s)

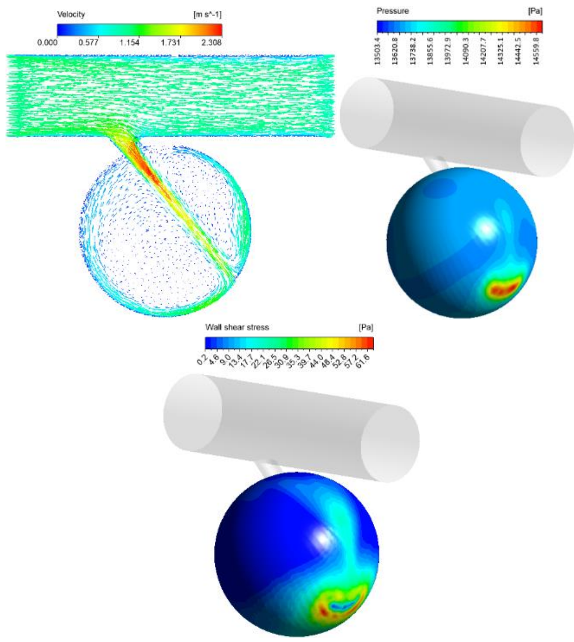

Figure 7. Velocity vectors in the midplane, pressure and wall shear stress on the aneursym surface (α=45˚, β=10˚, t=0.2 s)

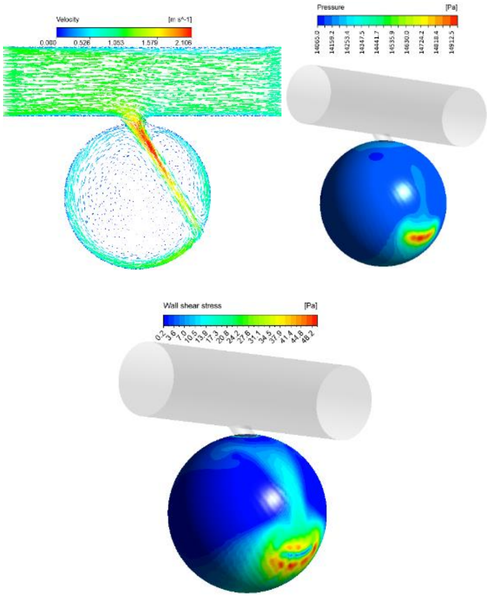

Figure 8. Velocity vectors in the midplane, pressure and wall shear stress on the aneursym surface (α=45˚, β=15˚

4. Conclusions

The results obtained because of the numerical analyzes for the different angle values between the neck region and the aneurysm (β) in a femoral pseudoaneurysm are summarized below,

- With the increase of the β angle, the blood flow velocity from the neck region decreased and the pressure on the surface of the aneurysm also decreased. The highest-pressure value in the aneurysm dome occurred for β =0˚.

- As with the pressure change, the lowest wall shear stress on the surface of the aneurysm was obtained at the β =15˚ angle, where the eccentricity of the neck axis and the aneurysm center point were the highest.

- When all the analysis results were evaluated, it was understood that for a pseudoaneurysm formed in the femoral artery, the highest growth rate and risk of rupture could occur at the β =0˚ angle.

With this numerical study presented, the growth rate and risk of rupture were tried to be analyzed depending on the growth position of the femoral pseudoaneurysm. It was predicted that the obtained findings will be beneficial in determining the treatment method and time in the treatment of femoral pseudoaneurysm.

5. Acknowledge

Ethics Committee Approval: Since it is a flow dynamics analysis study, there is no need for an ethics committee decision.
Informed Consent: Because of the retrospective design of the study, no informed consent form was obtained from patients.
Referee Evaluation Process: Externally peer reviewed.
Conflict of Interest Statement: The authors declare no conflicts of interest.
Financial Disclosure: The authors declared that this study has received no financial support.
Author Contributions: Authors declare that they all participated in the design, execution, and analysis of the manuscript and that they have approved the final version.

References

Mc Cann, R. L., Schwartz, L. B., & Pieper, K. S. (1991). Vascular complications of cardiac catheterization. *Journal of vascular surgery*, *14*(3), 375-381.

Cope, C., & Zeit, R. (1986). Coagulation of aneurysms by direct percutaneous thrombin injection. *American Journal of Roentgenology*, *147*(2), 383-387.

Franco, C. D., Goldsmith, J., Veith, F. J., Calligaro, K. D., Gupta, S. K., & Wengerter, K. R. (1993). Management of arterial injuries produced by percutaneous femoral procedures. *Surgery*, *113*(4), 419-425.

Hirano, Y., Ikuta, S., Uehara, H., Nakamura, H., Taniguchi, M., Kimura, A., ... & Ishikawa, K. (2004). Diagnosis of vascular complications at the puncture site after cardiac catheterization. *Journal of Cardiology*, *43*(6), 259-265.

Kim, H. H., Kim, K. W., Lee, C., Choi, Y. H., Kim, M. U., & Baba, Y. (2021). Percutaneous Thrombin Injection Based on Computational Fluid Dynamics of Femoral Artery Pseudoaneurysms. *Korean Journal of Radiology*, *22*(11), 1834.

Kronzon, I. (1997). Diagnosis and treatment of iatrogenic femoral artery pseudoaneurysm: a review. *Journal of the American Society of Echocardiography*, *10*(3), 236-245.

Krueger, K., Zaehringer, M., Strohe, D., Stuetzer, H., Boecker, J., & Lackner, K. (2005). Postcatheterization pseudoaneurysm: results of US-guided percutaneous thrombin injection in 240 patients. *Radiology*, *236*(3), 1104-1110.

Kurşun, B., Uğur, L., & Keskin, G. (2018). Hemodynamic effect of bypass geometry on intracranial aneurysm: A numerical investigation. *Computer Methods and Programs in Biomedicine*, *158*, 31-40.

Launder, B. E., & SD, B. (2013). MAN—ANSYS Fluent User's Guide Releasde 15.0. *Knowl. Creat. Diffus. Util*, *15317*, 724-746.

Lumsden, A. B., Miller, J. M., Kosinski, A. S., Allen, R. C., Dodson, T. F., Salam, A. A., & Smith 3rd, R. B. (1994). A prospective evaluation of surgically treated groin complications following percutaneous cardiac procedures. *The American surgeon*, *60*(2), 132-137.

Qiu, X. N., Fei, Z. M., Zhang, J., & Cao, Z. M. (2013). Influence of high-porosity mesh stent on hemodynamics of intracranial aneurysm: A computational study. *Journal of Hydrodynamics*, *25*(6), 848-855.

Sheiman, R. G., & Brophy, D. P. (2001). Treatment of iatrogenic femoral pseudoaneurysms with percutaneous thrombin injection: experience in 54 patients. *Radiology*, *219*(1), 123-127.

Shojima, M., Oshima, M., Takagi, K., Torii, R., Hayakawa, M., Katada, K., ... & Kirino, T. (2004). Magnitude and role of wall shear stress on cerebral aneurysm: computational fluid dynamic study of 20 middle cerebral artery aneurysms. *Stroke*, *35*(11), 2500-2505.

Siebert, M. W., & Fodor, P. S. (2009). Newtonian and non-newtonian blood flow over a backward-facing step–a case study. In *Proceedings of the COMSOL Conference, Boston* (p. 27).

Stone, P. A., Campbell, J. E., & AbuRahma, A. F. (2014). Femoral pseudoaneurysms after percutaneous access. *Journal of Vascular Surgery*, *60*(5), 1359-1366.

Suh, S. H., Kim, H. H., Choi, Y. H., & Lee, J. S. (2012). Computational fluid dynamic modeling of femoral artery pseudoaneurysm. *Journal of mechanical science and technology*, *26*(12), 3865-3872.

Yoo, T., Starr, J. E., Go, M. R., Vaccaro, P. S., Satiani, B., & Haurani, M. J. (2017). Ultrasound-guided thrombin injection is a safe and effective treatment for femoral artery pseudoaneurysm in the morbidly obese. *Vascular andendovascularsurgery*, *51*(6),3